Seismological Aspect of 26 December 2003 Bam Earthquake

Mehrdad Mostafazadeh, Amir Mansour Farahbod, Mohammad Mokhtari, and Mostafa Allamehzadeh

Seismology Research Center, International Institute of Earthquake Engineering and Seismology (IIEES), Tehran, Iran, email: mehrdad@iiees.ac.ir

ABSTRACT: *A waveform inversion algorithm, based on least square method, has been applied to the P and S waves of the 26 December 2003 Bam earthquake. The aftershocks of this event distributed along a narrow zone (approximately 20km) in N-S direction. In this research, estimates of centroid depth, seismic moment, and source mechanism have been obtained. The source mechanism derived from the inversion of long period body waves revealed that two events occurred on N-S trending strike-slip fault with a thrust component. According to the source model estimated in this study, the Bam earthquake was a multiple event. The rupture following the first event started at a depth of about 8km. However depth of the second event is about 10km. The total seismic moment estimated from inversion processes is 8.34×10^{18}Nm. The seismic moment of the second event is less than the first one (the seismic moment of second event is calculated as 2.34×10^{17}Nm). The pulse duration of main shock and the second event was determined from source time function and it is 1.7s and 0.8s respectively. Corner frequency and source radius have been calculated for main shock and the second event by using pulse duration. The range of corner frequency and source radius are from 0.187Hz -0.397Hz and 5.47km-2.57km for main shock and second event, respectively.*

Keywords: Bam; Seismicity; Error ellipse; Waveform modeling; Mainshock

1. Introduction

The 26 December 2003 Bam earthquake, *Mw* = 6.5, occurred at 01:56:56 *GMT*, in southeast of Iran, see Figure (1) near the city of Bam which had a population of about 100,000. The earthquake killed around 26500 people, destroyed and damaged more than 70 percent of buildings completely, and damaged the surrounding area. The strong motion record of the main shock indicates a peak horizontal and vertical acceleration of about 0.79*g* and 1.01*g* respectively [1] where the maximum intensity was assigned as *IX* (*EMS* 98 scale). This is generally accepted that the first aftershocks which occurring during the first 24 or 48 hours after the main shock defines the relevant rupture surface [2]. Based on this fact, from the first hours after the main shock, International Institute of Earthquake Engineering and Seismology (*IIEES*) started to locate the aftershocks using local and regional permanent seismic stations. The largest aftershock was located by *IIEES* during the first 2 days after the main shock had a magnitude of *Ms* = 5.1.

Using first motion analysis of P-wave or S-wave polarization provides a powerful tool in order to determine the most consistent orientation of a double couple mechanism which fits a number of observations. However such studies rarely constrain the focal mechanism tightly, since in many cases there are insufficient readings in many azimuths around the epicenter. Furthermore, the first arrivals describe only the early part of the source mechanism, which is not necessarily representative of the whole earthquake source process, and they give no information on the scalar moment. In the recent years, technical improvement for calculating synthetic seismograms and modeling the observed waveforms has become an important tool in the study of source mechanisms. The

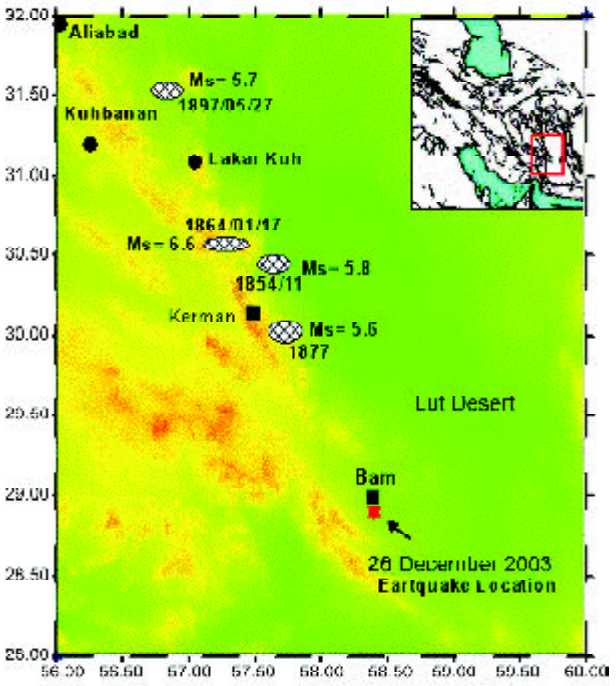

Figure 1. Map showing the location of 26 December 2003 main shock (star), Bam and Kerman city (black square), villages (black circle), and Historical event ( ).

methods of earthquake quantification have been developed for different phases and frequency bands way compare observed and theoretically predicted wave shapes and amplitudes. Although this information is of fundamental interest, it is desirable to know more about the spatial and temporal distribution of moment release. The teleseismic source time function gives information about fault ruptures or source complexity [3]. The principal purpose of this study is to determine the source characteristics, evaluate fault rupture or source complexity, and prepare information about time history of displacement on the Bam fault based on analysis of the three component waveform data from the far-field *GDSN* stations in the epicentral range 30°- 90°.

2. Historical and Instrumental Earthquakes

A study of historical earthquake records [4] shows that some of damaging earthquakes had occurred in Kerman province (the capital of Kerman province is Kerman city) while the Bam city itself experienced no great historical events during the past 2000 years. Figure (1) shows the location of some of historical events near the Bam city. The most significant events are:

The 27 May 1897 earthquake with magnitude M =5.7 which affected a larger area, caused damage in the Kerman. In 17 January 1864, the Chatrood earthquake (M = 6.0) occurred in the region. In April 1854, the Horjand earthquake (M = 5.8, I_o=*VIII*) occurred in northeast of Kerman. This catalogue shows that the earthquake had a same trend as Lakarkuh fault. In 1877 Sirch-Hasan-abad earthquake (M = 5.6) destroyed some of villages (Ab-e-garm, Sirch, Hasanabad, Deh-Gholi and Hashtadan villages). Figure (2) shows the location of the four major earthquakes with magnitudes of greater than 5.6 that have struck the cities and villages in the northwest of Bam during the period of 1981 to 1998. These events are listed bellow:

1. The Golbaf earthquake of 11 June 1981, *Ms*6.7,
2. The Sirch earthquake of 28 July 1981, *Ms*7.1,
3. The South Golbaf earthquake of 20 November 1989, *mb*5.6,
4. The North Golbaf (Fandogha) earthquake of 14 March 1998, *Mw*6.6.

Sirch earthquake is the largest event recorded instrumentally in the Kerman province. The large earthquakes in 1981 were associated with a total 64*km* of fresh movements along northern end of Golbaf (Gowk) fault and 10*km* at the southern segment of Lakarkuh fault. A maximum vertical displacement of 10*cm* were observed east of Golbaf, whereas after the second shock displacement of 14*cm* vertical and 20*cm* horizontal (Dextral) were measured near Chahar-Farsang and Poshteh along the Lakarkuh fault system [5].

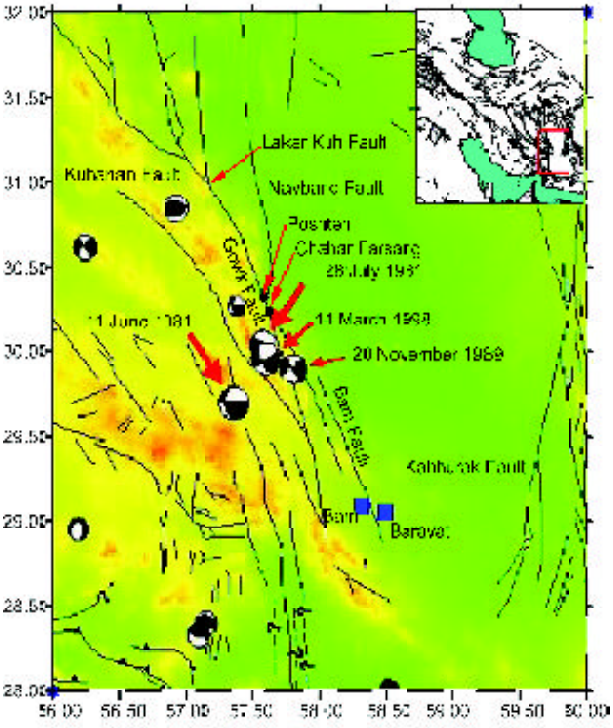

Figure 2. Moment tensor solutions (reported by CMT), fault Map of the Bam and surrounding area [6].

3. Aftershock Sequence

Following the Bam earthquake, *IIEES* recorded 158 aftershocks with magnitude between 2.0< *ML*<5.1 during the first month. For detailed study of the aftershocks nearly two days after the main event, *IIEES* deployed local temporary seismic stations in the epicentral area. This network consisted of nineteen medium-band and short period stations with an operating period of more than one month, starting December 28, 2003. Figure (3) shows the distribution of these events by the end of January 2004.

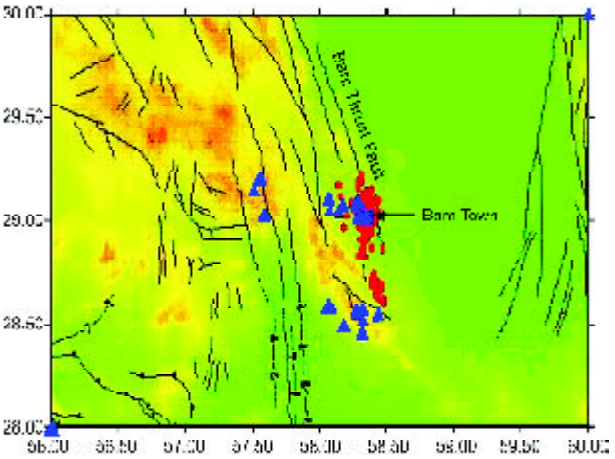

Figure 3. Map show distribution of temporary local stations (▲), aftershocks (●), and Bam city (■).

For locating the aftershocks we used *P* wave velocity model with a horizontal layered structure and with lateral variation of thickness of the upper-most layers was employed, which has been previously used by Zohoorian et al [5]. The parameters of horizontal layered structure are listed in Table (1). *S* wave velocities were calculated on the assumption that the V_p/V_s ratio is 1.73. More than three hundred Aftershocks having four or more *P* times were located and plotted as shown in Figure (3). In this view most part of the aftershocks for a length of about 20*km* closely follows the west of the Bam thrust fault. To get the local magnitude of each event, instrument correction and simulation of standardized instruments have been done using maximum peak-to-peak amplitudes [7]. The most part (75 percent) of these aftershock have magnitude range 1.0<*ML*<3.0. The ranges of depth of these aftershocks are changed between 6-20*km*.

Table 1. Initial model for the southern parts of the Kerman province (north of Bam) based on Zohoorian et al [5].

Layer	V_s (km/s)	D (km)
1	5.00	0.0
2	5.50	6.0
3	6.50	16.0
4	8.00	41.0

4. Evaluate of Errors in Location Coordinate and Error Ellipsoid of the Larger Aftershocks

Evaluate of discrepancies in location parameter and error area for common events (aftershocks) reported by the International Data Center (*IDC*), and *IIEES* are show in Figures (4) and (5).

The Minimum and Maximum *IDC* Error ellipse area are changed 105Km^2 to 530Km^2 (in *REB* bulletin).The minimum and maximum misslocation between the far-field (*IDC*) and near field (*IIEES*) data are 79*km* and 92*km*, respectively shown in Figure (5).

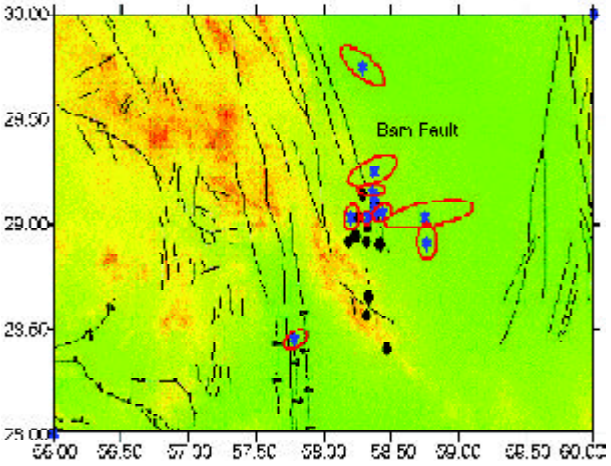

Figure 4. The Map shows epicenter error area (-.-.-) reported by International Data Center (IDC), and the location of epicenter reported IIEES.

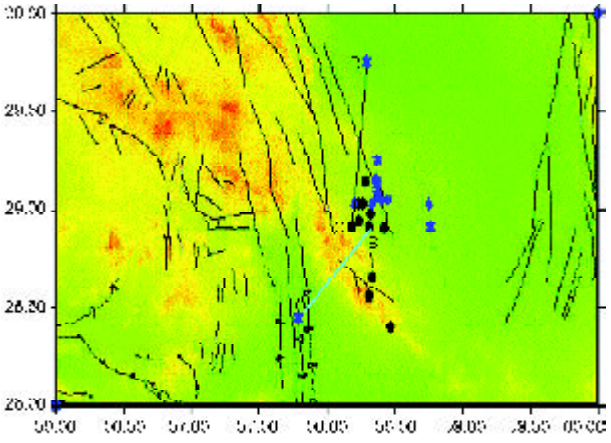

Figure 5. The map shows maximum and minimum Miss location of the epicenter reported by IIEES (●) and IDC (✱), location difference, 79km A——B and location difference, 92km C——D .

5. Waveform Inversion of Body Waves and Source Parameters

Body wave modeling has become one of the most important tools available to seismologist for refining earth structure models and understanding fault-rupturing process. Both *P*- and *SH*- were used to constrain earthquake source parameters. We compared the shapes and amplitudes of long-period *P*- and *SH*- wave recorded by *GDSN* stations. *IASPEI SYN*4 algorithm [8], which is a recent version of Nabelek's [9] inversion procedure based on a weighted least squares method, was used for waveform inversion. The source time function (described by a series of overlapping isosceles triangles) [8], centroid depth, and the fault orientation parameters (strike, dip, and the rake) are used in order to compute synthetic seismograms and the seismic moment.

The inversion procedure adjusts the relative amplitudes of the source time function element, the centroid depth, the seismic moment and source orientation. This solution has been referred as the minimum misfit solution. The Green's function for *P* and *SH* waves can be express in the form [10]:

$$g(t)=CR(t)*M(t)*g^{S}(t) \quad (1)$$

Where $g^{S}(t)$ is the displacement of the *P* or *SH* waves emerging at the base of the crust in the source region in response to a impulse, $M(t)$ and $CR(t)$ are the responses to these waves by the mantle and crust at the receiver respectively.

Amplitudes which are corrected for geometrical spreading and attenuation is introduced with a $t^*=1s$ for *P* wave and $t^*= 4s$ for *SH* wave [9]. As explained by Fredrich [12], uncertainties in t^* effect the source duration and seismic moment, rather than the source orientation or centroid depth.

The seismic moment clearly depends on the duration of the source time function, and to some extends on centroid depth and velocity structure [12]. As the main interest was on source orientation and depth, we did not concern much with uncertainties in seismic moment, which in most cases are probably about 30 per cent. The lengths of a time function was estimated by increasing the number of isosceles triangles until the amplitudes of the later ones became insignificant.

6. Uncertainties in Source Parameters

Having found a set of acceptable source parameters, the procedure described by MaCaffrey and Nabelek [11], Fredrick et al [12], and Taymaz [10] was followed, in which the inversion routine is used to carry out experiments to test how well individual source parameters are resolved. One parameter at a time was investigated by fixing it at a series of values either side of its value yielded by the minimum misfit solution, and allowing the other parameters to be found by the inversion routine. The quality of fit between observed and synthetic seismograms was then visually examined to see whether it had deteriorated from the minimum misfit solution. In this way we were able to estimate the uncertainty in strike, dip, rake and depth for each event. In common with the authors cited above, we believe this procedure gives a more realistic quantification of likely errors than the formal errors derived from the covariance matrix of the solution (strike test is show in Figure (6)).

Uncertainties in seismic moment and centroid depth arise from errors in the source velocity model. The crustal structure at the source and receiver is modeled as a single layer over a half space. The material constants assumed for region are $V_P = 6.5 km\ s^{-1}$, $V_s = 3.7 km\ s^{-1}$ and $\rho = 2.9 gr.cm^{-3}$.

A number of automatic preliminary *CMT* solutions for Bam earthquake have been reported by *USGS-PDE* and the others. Among them the best double-couple fault plane solutions determined by Harvard. While all solutions show dominant strike slip faulting. Long-Period body wave seismograms were inverted to obtain a detailed fault mechanism solution and source parameters of the 26 December 2003 Bam earthquake. In the distance range of about 30°-90° $M(t)$ includes only the effects of an-elastic attenuation, geometrical spreading and travel time. Body waves propagate steeply (15°-35° from the downward vertical) through the crust and uppermost mantle and are therefore influenced mostly by the vertical structure below the source and receiver [10].

In this reason good quality *GDSN* long period P-waves and S-waves recorded in the distance range of 30°-90° were selected. All waveforms were low-pass filtered (Butterworth) at a cut of frequency of $0.2 Hz$ in order to remove the high frequency component which may cause instability during the inversion. When the *P* waveforms were examined prior to the inversion procedure, it was recognized that the occurrence of a second source with a considerable delay time is quite probable. The source parameters of inversion process are given in Table (2). The minimum misfit solution for the main shock is shown in Figure (7). According to direction of local

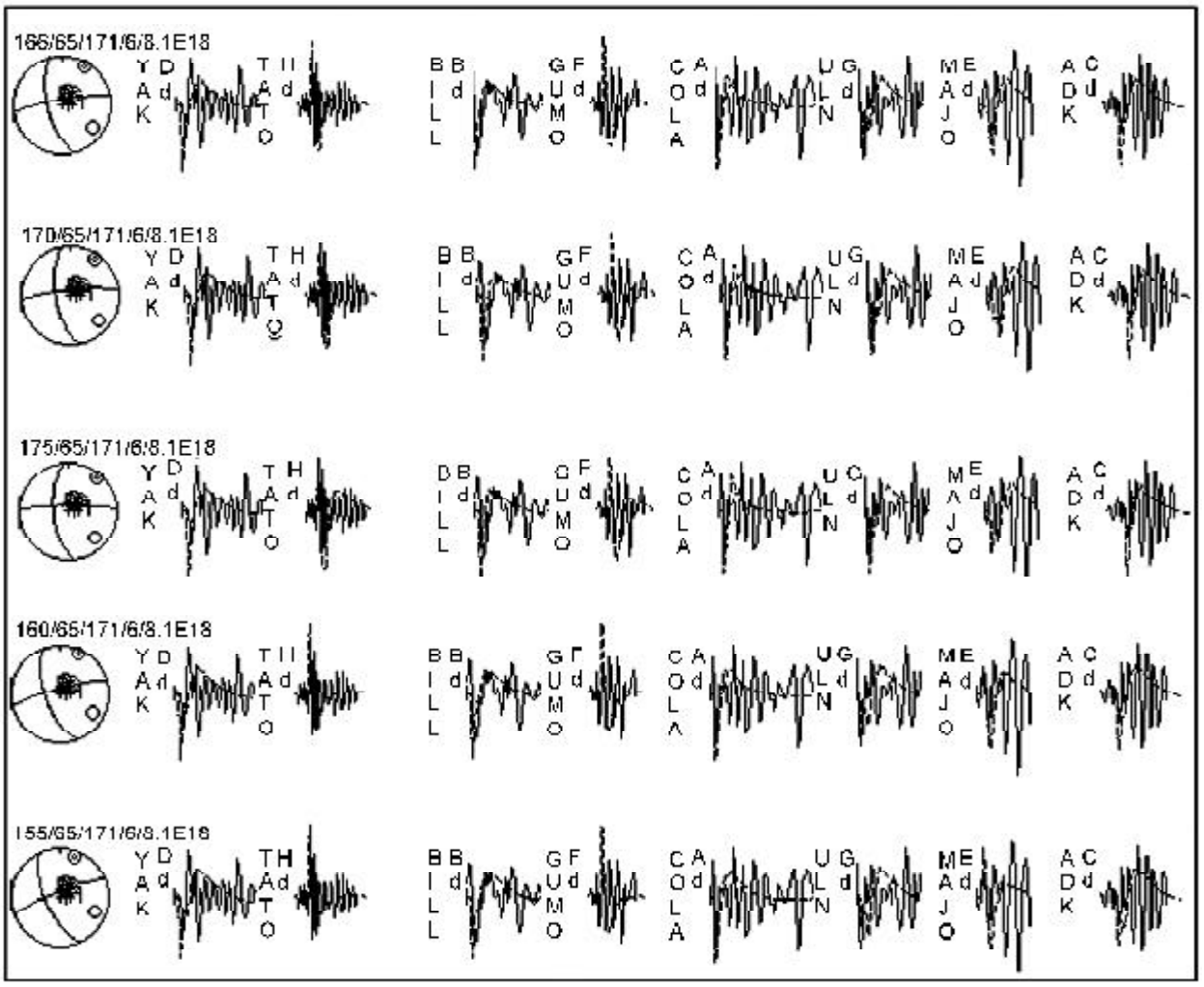

Figure 6. In this each row shows a selection of waveforms from a run of the inversion program. At the start of each row is the P focal sphere for the focal parameters represented by the five numbers (strike, dip, rake, depth and moment. The station code is identified to the left of each waveform. Observed waveform (solid lines) and synthetic data (dotted lines) shown in this figure.

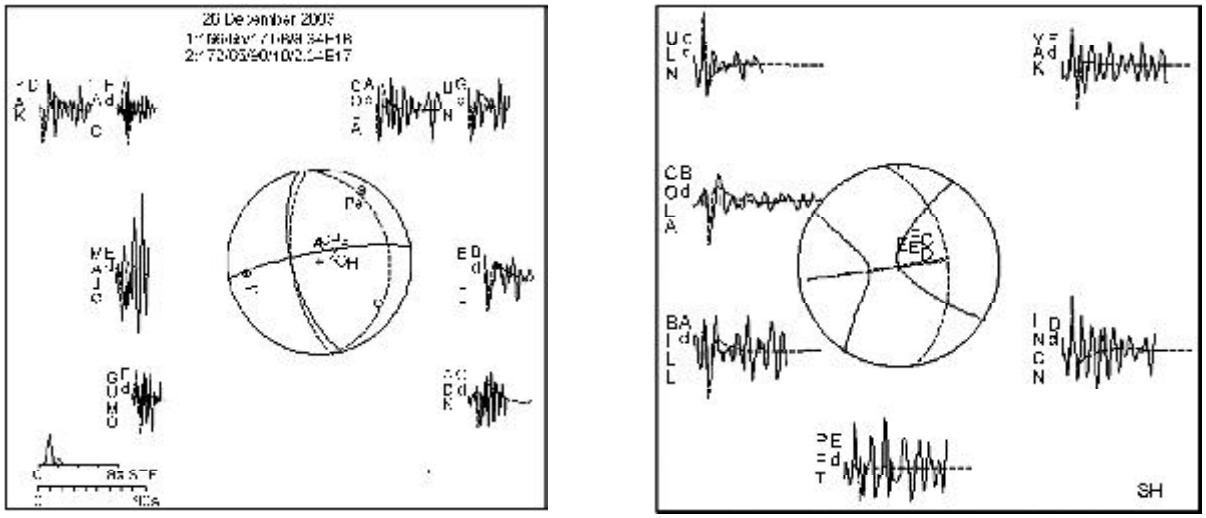

Figure 7. The P and SH radiation patterns of minimum misfit solutions for the earthquake of26.12. 2003 main shock are shown in this figure. Observed waveform (solid lines) and synthetic data (dotted lines), source time function shown in this figure. The compression (Ps, Pt points for strike slip and thrust component fault respectively) and dilatation axes are marked by solid and open circle respectively. The station code is identified to the left of each waveforms, and lower case letter that indicates the type of instrument (d= GDSN long period).

Table 2. Source parameters of the 26 December 2003 Bam earthquake.

Nodal plane 1				Nodal Plane 2			
Source No	Strike (o)	Dip (o)	Rake (o)	Strike (o)	Dip (o)	Centroid Depth (km)	M_o (Nm)
1	166±10	36±8	17±5	260±7	81±10	7.9±4	8.34e+18
2	172±9	65±12	90±-	352±6	25±12	10±6	2.34e+17

faults in area, see Figure (2) [18], displacement observations in the field [19] and aftershocks distribution, we think the nodal plane one is the main strike slip fault.

7. Source Time Function

The teleseismic source time function gives information about fault ruptures or source complexity. The physical features of teleseismic source time functions appraise the source complexity of the earthquakes. These features include the overall duration, multiple or single event character, individual source pulse widths, and roughness of the time function. The measures of source size and complexity can then be compared with the plate convergence rate, and other physical parameters in collision zone [3]. The earthquakes larger than about M_s6.9 can rarely be represented by a single point source, even at the wavelengths recorded by the *WWSSN* 15-100 long period instruments (with a peak response at a bout 15*s* period). These earthquakes usually consist of several discrete ruptures, separated by several seconds in time and several km in space, often occurring on faults with different orientations [13]. From the source time function it appears that the rupture broke two asperities in the total rupture time 3*s*, see Figure (8). The seismic moment of the second event was less than the first one. We estimated the corner frequency is very approximately given by $f_0 = 1/\pi\tau_p$ where τ_p is the largest pulse duration [14, 15]. The essential purpose of calculating the corner frequency is evaluating the source dimension. Then we have calculated source radius using [16] relation for a circular fault, see Table (2). We used 2.75*km*/*sec* for rupture velocity [17].

$$R = 2.34v/2\pi f_0 \qquad (2)$$

The seismic moment, M_o, is given by $M_o = \mu.A.\hat{u}$, where μ is the rigidity ($\sim 3\times10^{10}Nm$), A is the fault area, and $\hat{u}$ is the average displacement in source, see Table (3). Average displacement in source was calculated by using source time function.

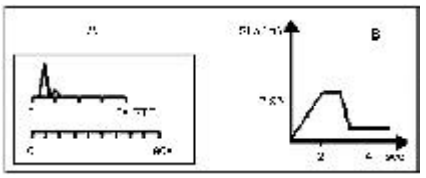

Figure 8. The source time function (A) and average displacement (B) in the source.

Table 3. Source parameters that are obtained from source time function.

Source No.	Pulse Duration τ_p (sec)	Corner Frequency f_0 (Hz)	Source Radius r_0 (km)	Source Area (km^2)	Displacement in Source (m)
1	1.7	0.187	5.47	93.99	2.95
2	0.8	0.397	2.57	20.74	0.35

8. Discussion and Conclusion

The mechanism of the 26 December 2003 earthquake derived from the inversion of long period body waves and field observations comprises a strike-slip solution. In addition we have derived thrust component for this earthquake but we have not found any clear geologic surface data in the field. The geological observations suggest that the essential fracturing is occurred in broad zone with diameter 9*km* and width 4*km* in south to north of Bam. According to focal mechanism, no surface faulting observation [19] aftershocks distribution, it is assumed that this fault has *N-S* trend in south of Bam and it has blind characteristic. Varying the seismic moment along total duration of *STF* is direct the related to the variation the source velocity structure did have an effect on centroid depth and seismic moment. In addition uncertainties in attenuation factor, *t**, mainly affect estimates of source duration and seismic moment. The centroid depth of main shock is less than second event. We can see clearly in the source time function this earthquake has larger moment release in the first part of the process with respect to the second event. In addition the source dimension of second event is less than main shock, see Table (3). The nature of this function shows that the faulting consists of several fractures separated by strong barriers. In conjunction with the spatial and temporal behavior of this event the complexity of rupture suggests that strain accumulated gradually on a system of fault in different geological structure. The effect of a critical rupture (the first event of the main shock) was to cause a rapid release of stress (dominant event of the main shock) as well as a more gradual release of stress (the second event) on adjacent conjugate fault.

Acknowledgment

We are grateful to Prof. Mohsen Ghafory Ashtiany for his supports, all anonymous reviewers for review and discussion and other colleagues at *IIEES* for their efforts concerning the installation of local temporary seismic network in the Bam area.

References

1. Zare, M. and Hamzeloo, H. (2004). "Study of Strong Ground Motion Data for the 2003 Bam Earthquake", SE Iran, Published in This Issue.
2. Kisslinger, C. (1997). "Aftershocks and Fault Zone properties", *Advances in Geophysics*, **38**, 1-35.
3. Hartzell, S. and Heaton, T. (1985). "Teleseismic Time Functions for Large, Shallow Subduction Zone Earthquakes", *Bull. Seism. Soc. Am.*, **75**(4), 965-1004.
4. Berberian, M. (1994). "Natural Hazards and First Earthquake Catalogue of Iran, V.1. Historical Hazards in Iran Prior to 1900", International *Institute of Earthquake Engineering and Seismology (IIEES)*, P.603
5. Zohoorian, A.A., Mohajer-Ashjai, A., Kabiri, A., and Hosseinian-Ghamsari, M. (1984). "Damage Distribution and Aftershock Sequence of Two Destructive Earthquakes in 1981 in Eastern Kerman", *J. Earth and space phys.*, **10**(1, 2).
6. Cornel University, Building Digital Earth Project, Institute for the Study of Continent (INSTOC) Cornell University.
7. Hutton, L.K. and D. Boore (1987). "The ML Scale in Southern California", *Bull. Seism. Soc. Am.*, **77**, 2074-2094.
8. McCaffery, R., Abers, G., and Zwick P. (1991). "Inversion of Teleseismic Body Waves", In: Digital Seismogram Analysis and Waveform Inversion (ed. By W. H. K. Lee), IASPEI software Library, **3**, 81-166.
9. Nabelek, J.L. (1984). "Determination of a Earthquake Source Parameters from Inversion of Body Waves", Ph.D. Thesis, MIT, Cambridge Massachusetts.
10. Taymaz, T. (1990). "Earthquake Source Parameters in the Eastern Mediterranean Region", Ph.D. Thesis., Drawing college Cambridge.
11. McCaffrey, R. and Nabelek, J. (1987). "Earthquakes Gravity, and the Origin of the Bali Basin: an Example of a Nascent Continental Fold-and-Thrust Belt, *J.Geophys. Res.*, **92**, 441-460.
12. Fredrick, J., McCaffrey, R., and Denham, D. (1988). "Source Parameters of Seven Large Australian Earthquakes Determined by Body Waveform Inversion", *Geophys. J.*, **95**, 1-13.
13. Butler, R., Stewart, G.S., and Kanamori, H. (1979). "The July 27 1976 Tangshan China Earthquake -a Complex Sequence of Intraplate Events, *Bull. Seism. Soc. Am.*, **69**, 207-220.
14. Helmberger, D.V. and Malone, S.D. (1975). "Modeling Local Earthquakes as Shear Dislocations in a Layered Half-Space, *J. Geophys. Res.*, **80**, 4881-4888.
15. Husebye, E.S. and Mykkeltveit, S. (1980). "Identification of Seismic Sources Earthquake or Underground Explosion. Proceeding of the NATO Advanced Study Institute Held at Voksenasen", Oslo, Norway, 72-97.
16. Brune, J.N. (1970). "Tectonic Stress and the Spectra of Seismic Shear Waves from Earthquakes, *J. Geophys. Res.*, **75**, 4997-5009.
17. Hartzel, S., Langer, C., and Mendoza, C. (1994). "Rupture Histories of Eastern North American Earthquakes", *Bull. Seism. Soc. Am.*, **84**(6), 1703-1772.
18. Berberian, M., Jackson, J.A., Fielding, E., Parsons, B, E., Priestley, K., Qorashi, M., Talebian, M., Walker, R., Wright, T.J., and Baker, C. (2001). "The 1998 March 14 Fandooqa Earthquake (Mw6.6) in Kerman Province, Southeast Iran: Re-Rupture of the 1981 Sirch Earthquake Fault, Triggering of Slip on Adjacent Thrust and Active Tectonics of the Gowk Fault Zone, *Geophys. J. Int.*, **146**, 371-398.
19. Hessami, K., Tabassi, H., Okumura, K., Azuma, T., Echigo, T., Kondo, H., and Abbassi, M.R. (2004). "Surface Expression of Bam Fault Zone in Southeastern Iran: Causative Fault of the December 26, 2003 Earthquake", Press in this Volume.